Nuclear Physics B275 [FS17] (1986) 375–397
North-Holland, Amsterdam

THE COMPLEX LANGEVIN EQUATION AND MONTE CARLO SIMULATIONS OF ACTIONS WITH STATIC CHARGES*

J. AMBJØRN

The Niels Bohr Institute, University of Copenhagen, Blegdamsvej 17, DK-2100 Copenhagen Ø, Denmark

M. FLENSBURG and C. PETERSON

Department of Theoretical Physics, University of Lund, Sölvegatan 14 A, S 22362 Lund, Sweden

Received 14 April 1986

We explore the possibilities of using the complex Langevin equation to Monte Carlo generate configurations of gauge theories with static charges present in the action. Successful results are obtained for systems that possess nontrivial saddle-point (classical) solutions. For that reason the algorithm works impressively for two-dimensional U(1) in the entire β-range whereas for three- and four-dimensional U(1) the applicability is limited to the weak coupling regime (large β). The method fails completely for SU(2) and SU(3).

1. Introduction

It is often convenient to be able to make Monte Carlo simulations of systems described by complex (effective) actions. Most notable is of course the desire to simulate physical processes without having to rotate from Minkowski space to euclidean space [1]. But even in euclidean field theory one frequently encounters situations, where the effective actions are complex. The integration over fermionic degrees of freedom, the inclusion of topological terms or chemical potentials or certain external fields can generate complex effective actions when rotated from Minkowski space-time to euclidean space [2–6].

In these cases most standard Monte Carlo updating techniques, like Metropolis and the heat bath, cannot be used in a straightforward manner. Even the measurement of the simplest "internal" observables can become exceedingly difficult since one has to include the imaginary part of the action in the measurement. If the action can be written as

$$S(\theta) = S_{\mathrm{R}}(\theta) + S_{\mathrm{I}}(\theta), \tag{1.1}$$

* Work supported in part by the Swedish Natural Science Council under contract NFR F 7017-109.

where S_R and S_I denote the real and imaginary parts, respectively, the expectation value of an observable $O(\theta)$ is in terms of the action $S(\theta)$ given by

$$\langle O(\theta)\rangle_S \equiv \frac{\int D\theta\, O(\theta) e^{-S(\theta)}}{\int D\theta\, e^{-S(\theta)}}, \tag{1.2}$$

$$\langle O(\theta)\rangle_S \equiv \frac{\langle O(\theta) e^{-S_I(\theta)}\rangle_{S_R}}{\langle e^{-S_I(\theta)}\rangle_{S_R}}, \tag{1.3}$$

$$\langle Q(\theta)\rangle_{S_R} \equiv \frac{\int D\theta\, Q(\theta) e^{-S_R(\theta)}}{\int d\theta\, e^{-S_R(\theta)}}. \tag{1.4}$$

In principle eqs. (1.3) and (1.4) allow for the calculation of $\langle O(\theta)\rangle_S$ by standard methods if $S_R(\theta)$ is not too pathological. (Note that S_R is zero in Minkowski space.) The problem with the method is that S_I grows as the linear size of the system increases. For large volume or strong coupling both $\langle\ \rangle_{S_R}$ expectation values in eq. (1.3) become very small and the determination of $\langle O(\theta)\rangle$ by this method becomes impossible from a practical point of view. By using S_R only in the updating procedure we are generating *irrelevant* configurations. How much more efficient would it be if one could generate the relevant configurations with "probability distributions" corresponding to $e^{-S(\theta)}$. Since $S(\theta)$ is complex, a conventional probability distribution of $e^{-S(\theta)}$ is not possible. This is why the standard methods for generating probability distributions do not work.

The Langevin equation (which of course should be included in the list of standard Monte Carlo techniques) offers a way to circumvent this difficulty, as first realized by Klauder [2], and Parisi [7]. It can be written as

$$\dot{\theta}(t) = -\frac{\delta S(\theta)}{\delta\theta} + \eta(t), \tag{1.5}$$

where $\eta(t)$ is a gaussian noise, appropriately normalized. For ordinary real actions, eq. (1.5) can be used to generate the configurations $\theta_\eta(t)$, and the stochastic average of the observable $O(\theta)$ can be defined according to

$$\langle O(\theta(t))\rangle_\eta = \frac{\int D\eta(\tau)\, O(\theta_\eta(t)) \exp\left(-\frac{1}{4}\int_0^\infty d\tau\, \eta^2(\tau)\right)}{\int D\eta(\tau) \exp\left(-\frac{1}{4}\int_0^\infty d\tau\, \eta^2(\tau)\right)}. \tag{1.6}$$

It follows from standard treatments of the Langevin equation that

$$\langle O(\theta)\rangle_S = \lim_{t\to\infty} \langle O(\theta(t))\rangle_\eta \tag{1.7}$$

and ergodicity leads to

$$\langle O(\theta)\rangle = \lim_{T\to\infty} \frac{1}{T}\int_0^T \mathrm{d}t\, O\big(\theta_\eta(t)\big). \tag{1.8}$$

The observation by Klauder [2], and Parisi [7] was that even if $S(\theta)$ is complex eq. (1.5) can be solved and a stochastic average like in eqs. (1.6)–(1.8) formally defined. If this approach would work without problems it seems that a way to generate the effective "probability distribution" $\mathrm{e}^{-S(\theta)}$ has been found and the gains would be tremendous.

It is the purpose of this article to point out that:

(i) Indeed there exist situations where the method works beautifully and allows us to measure quantities which by conventional methods would be just impossible to measure since they would according to eqs. (1.3) and (1.4) involve ratios between quantities which individually could be of the order $O(10^{-100})$.

(ii) The approach might fail and give wrong physics in some situations. Hence it may be dangerous to use the method in situations where one explores new areas of physics and our intuition may not be trusted.

This paper is organized as follows: In sect. 2 we discuss the complex Langevin equation and in what sense it generates the "probability distribution" $\mathrm{e}^{-S(\theta)}$ when $S(\theta)$ is complex. We formulate the complex Langevin equation for abelian and non-abelian gauge theories and discuss the non-trivial problem of convergence. This problem has both a theoretical and a practical numerical part that need to be addressed.

In sects. 3 to 6, we discuss the measurement of the field strengths between charged particles in lattice QED and QCD in the quenched approximation. The measurement of the string tension in lattice QCD has received great attention. It is obviously one of the more fundamental quantities to measure. However the attempts to make precise measurements on the string tensions so far have been hampered by the difficulties mentioned in connection with eqs. (1.2)–(1.4). The conventional Monte Carlo techniques used in lattice gauge theories can only generate an ensemble of vacuum configurations of which most are *irrelevant* for the static quark-antiquark potential. Consequently one has to use projectors like Wilson loop averages $W(R\cdot T)$ whose expectation values vanish exponentially for R or T large. If we want information about the physical string between the charges, its spatial extension and the fall-off of the field strengths away from the string, the situation is even worse. It requires the measurement of the correlation between a plaquette (the local energy density) and a Wilson loop divided by the expectation value of $W(R\cdot T)$:

$$\varepsilon_\square = \frac{\langle \mathrm{Tr}\, U_\square \mathrm{Tr}\, W(R\cdot T)\rangle - \langle \mathrm{Tr}\, U_\square\rangle\langle \mathrm{Tr}\, W(R\cdot T)\rangle}{\langle \mathrm{Tr}\, W(R\cdot T)\rangle}. \tag{1.9}$$

The problems associated with a measurement of $\varepsilon_\square$ by means of eq. (1.9) are exactly the ones described in connection with eqs. (1.3)–(1.4). If we could generate configurations in the charged sector of the theory by including the Wilson loop in the action the situation would be very different. The (confining) flux string between the charges would then have a constant energy density no matter how far they are separated (if we ignore the weakening due to the string vibration) and $\varepsilon_\square$ in eq. (1.9) could be measured as the expectation value of a plaquette. However, the euclidean action for a gauge theory with static charges included in the action is complex and as discussed above not suitable for standard Monte Carlo techniques. The complex Langevin equation therefore enters as a natural candidate for this kind of problem.

In sect. 3 we report on simulations for two-dimensional U(1). In this case the complex Langevin equation works quite well and the potential power of the method is revealed. However the next three sections describe various degrees of disasters that seem to occur in more complicated situations: sect. 4 addresses lattice U(1) in three and four euclidean dimensions. It turns out that the complex Langevin equation works impressively in the weak coupling regions but fails to produce the correct physics in the confining strong coupling regimes. In sect. 5 we describe some quantum mechanical examples where the method again fails at strong couplings. Unfortunately these examples are very relevant for the inclusion of Wilson loops in non-abelian gauge theory actions. The problems appearing here are briefly touched upon in sect. 6. Finally sect. 7 contains a discussion and an outlook.

2. The complex Langevin equation in lattice gauge theories

The complex Langevin equation is given by eq. (1.5). By a complex action $S(\theta_i)$ we have in mind a complex function of the real variables θ_i (if θ_i is a complex field we view it as two real fields: $\mathrm{Re}\,\theta_i$ and $\mathrm{Im}\,\theta_i$) that can be extended to a function on a Riemann surface. Furthermore we assume that $\exp(-S(\theta_i))$ is integrable and that the noise $\eta_i(t)$ is real. It is necessary to consider S as a function of the complex variable $\theta_i^z = \theta_i^x + i\theta_i^y$ because the solution of eq. (1.5) will generate a complex solution $\theta_\eta^z(t)$, even if $\eta(t)$ is real and $\theta_\eta(t=0)$ is real, as long as $\delta S(\theta)/\delta\theta_i$ takes complex values.

When written in terms of θ_i^x and θ_i^y, eq. (1.5) becomes an ordinary Langevin equation of real variables:

$$\dot{\theta}_i^x = -\mathrm{Re}\left[\frac{\delta S(\theta^z)}{\delta\theta_i}\right]_{\theta_i^z=\theta_i^x+\theta_i^y} + \eta_i(t), \tag{2.1a}$$

$$\dot{\theta}_i^y = -\mathrm{Im}\left[\frac{\delta S(\theta^z)}{\delta\theta_i^z}\right]_{\theta_i^z=\theta_i^x+i\theta_i^y}, \tag{2.1b}$$

and by the well-known relation between the Langevin equation and the Fokker-Planck equation we have for observables O which are *analytic* functions of θ_i

$$\left\langle O(\theta_i^z(t))\right\rangle_\eta = \int \prod_i \mathrm{d}\theta_i^x\, \mathrm{d}\theta_i^y\, O(\theta_i^x + i\theta_i^y)\, P(\theta_i^x, \theta_i^y; t)\,. \tag{2.2}$$

The positive definite probability distribution $P(\theta^x, \theta^y; t)$ is the one obtained by solving the Fokker-Planck equation corresponding to eq. (2.1):

$$\dot{P} = \frac{\delta^2}{\delta\theta_i^{x^2}} P - \frac{\delta}{\delta\theta_i^x}\left(v_{\theta_i^x} P\right) - \frac{\delta}{\delta\theta_i^y}\left(v_{\theta_i^y} P\right), \tag{2.3a}$$

$$v_{\theta_i^x} \equiv -\mathrm{Re}\left[\frac{\delta S(\theta^z)}{\delta\theta_i^z}\right]_{\theta_i^z = \theta_i^x + i\theta_i^y}, \tag{2.3b}$$

$$v_{\theta_i^y} = -\mathrm{Im}\left[\frac{\delta S(\theta^z)}{\delta\theta_i^z}\right]_{\theta_i^z = \theta_i^x + i\theta_i^y}. \tag{2.3c}$$

The relation to the complex "probability distribution" of the *real* variables θ_i in $\mathrm{e}^{-S(\theta_i)}$ comes about as follows: If we insist that the stochastic average of eq. (2.2) can be written as an integral over *real* fields θ_i one obtains

$$\left\langle O(\theta_i^z(t))\right\rangle_\eta = \int \prod_i \mathrm{d}\theta_i\, O(\theta_i)\, P(\theta_i; t)\,. \tag{2.4}$$

It is not too complicated to show, by applying the Langevin equation on the l.h.s. of eq. (2.4), that (see refs. [6] and [8] for details) $P(\theta_i; t)$ must satisfy

$$\dot{P}(\theta_i; t) = \frac{\delta^2}{\delta\theta_i^2} P(\theta_i; t) - \frac{\delta}{\delta\theta_i}\left(\frac{\delta S}{\delta\theta_i}\right) P(\theta_i; t)\,. \tag{2.5}$$

We recognize the Fokker-Planck equation *but with S complex*. If the imaginary part is sufficiently small it might still be argued that [9]

$$P(\theta_i; t) \underset{t\to\infty}{\to} \mathrm{e}^{-S(\theta_i)} \tag{2.6}$$

as desired, but we must stress that there exist no general theories which ensures this. In principle $P(\theta_i; t)$ is determined from eqs. (2.2) and (2.4) and by taking moments

one gets [6, 8]

$$P(\theta_i; t) = \frac{1}{2\pi} \int \prod_1 \mathrm{d}\xi_i \, \mathrm{e}^{-i\theta_i \xi_i} \left\langle \exp\left(i\xi_i \theta_i^z(t)\right)\right\rangle_\eta . \tag{2.7}$$

Eqs. (2.2) and (2.4) are addressing the general question of representing an indefinite kernel $P(\theta_i)$ by a positive definite one. The indefinite characters of $P(\theta_i)$ are transferred to the observable $O(\theta_i)$ by going from eqs. (2.4) to (2.2). $O(\theta_i)$ cannot be positive definite in the whole complex plane, being an analytic function. In the following we are going to be interested mainly in lattice gauge theories with Wilson lines included in the time direction and separated in space by a distance R. We will use periodic boundary conditions in the time direction with period T.

In the abelian case the partition function can be written

$$Z(\beta, L_1, L_2) = \int \prod_{n,\mu} \mathrm{d}\theta_{n,\mu} \exp\left(\beta \sum_{\square} \cos\theta_{\square}\right) W(L_1) W^{-1}(L_2), \tag{2.8}$$

where

$$\theta_{\square_{n;\mu\nu}} \equiv \theta_{n,\mu} - \theta_{n,\nu} - \theta_{n+\hat{\nu},\mu} + \theta_{n+\hat{\mu},\nu}, \tag{2.9}$$

$$W(L) = \prod_{\ell \in L} \mathrm{e}^{i\theta_\ell}; \qquad \ell \equiv n, d. \tag{2.10}$$

The euclidean direction d is taken as the time direction. In fig. 1 this is illustrated for $L_1 - L_2 = 2$ and $d = 2$.

The non-abelian analog of eq. (2.8) for the group SU(N) is given by

$$Z(\beta, L_1, L_2) = \int \left(\prod_{n,\mu} \mathrm{d}U_{n,\mu}\right) \exp\frac{\beta}{2N} \mathrm{Tr}\left(U_{\square} + U_{\square}^{-1}\right)$$

$$\times \frac{1}{N} \mathrm{Tr}\, W(L_1) \frac{1}{N} \mathrm{Tr}\, W(L_2)^{-1}, \tag{2.11}$$

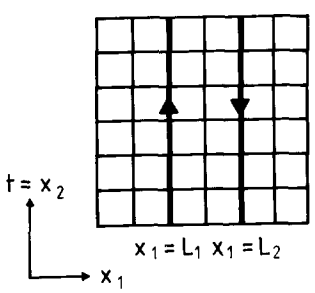

Fig. 1. Wilson lines in the time direction located at L_1 and L_2.

where

$$U_{\square_{n,\mu\nu}} \equiv U_{n,\mu} \cdot U_{n,\nu}^{-1} \cdot U_{n+\hat{\nu},\mu}^{-1} \cdot U_{n+\hat{\mu},\nu}, \tag{2.12}$$

$$W(L)_{n_0} \equiv U_{n_0+(T-1)\hat{d},d} \cdot U_{n_0+(T-2)\hat{d},d} \cdots U_{n_0,d}. \tag{2.13}$$

$W(L)_{n_0}$ is the product of the T link variables belonging to the line L starting with the link n_0, d. (L is a Wilson line in the time direction d).

We should note that some care has been taken in order to use U^{-1} instead of U^+ in the formulae for the action. The reason is that for the complex Langevin equation U will no longer take values in SU(N) but rather in its complex extension SL(N,C). The action thus becomes an analytic function of $U \in \mathrm{SL}(N,\mathrm{C})$ only if U^{-1} is used as a variable.

The effective action can now be written as

$$S = \beta \sum_{\square} \cos\theta_{\square} + i\Big(\sum_{\ell \in L_1} \theta_\ell - \sum_{\ell \in L_2} \theta_\ell \Big) \tag{2.14}$$

in the abelian case and

$$S = \frac{\beta}{2N} \mathrm{Tr}\big(U_{\square} + U_{\square}^{-1}\big) - \log \mathrm{Tr}\, W(L_1) - \log \mathrm{Tr}\, W(L_1)^{-1} \tag{2.15}$$

in the non-abelian case. The Langevin equations can now be written down. In the abelian case (1.5), eq. (2.14) immediately gives

$$\dot{\theta}_\ell = -\beta \sum_{\ell \in \square} (\square|\ell) \sin\theta_{\square} + i\big(\delta_{\ell,L_1} - \delta_{\ell,L_2}\big) + \eta_\ell, \tag{2.16}$$

where ℓ is a link variable ($\ell \equiv n, \mu$) and $(\square|\ell) = \pm 1$ depending on the orientation of the plaquette relative to the link $\ell \in \square$. In the non-abelian case some additional notation is needed (we refer to ref. [6] and references herein for details). Let T^a denote the anti-hermitian generators of SU(N), normalized according to

$$\mathrm{Tr}\, T^a T^b = -\tfrac{1}{2}\delta^{ab} \tag{2.17}$$

and ∇_ℓ^a; the right Lie derivate on SU(N)

$$\nabla_\ell^a = i(U_\ell T^a)_{ij} \frac{\delta}{\delta (U_\ell)_{ij}}, \qquad \ell \equiv n, \mu. \tag{2.18}$$

The Langevin equation on SU(N) can now be written as

$$U_\ell^{-1} \dot{U}_\ell = -T^a \nabla_\ell^a S(U_\ell) + T^a \eta_\ell^a. \tag{2.19}$$

For the action $S(U_l)$ given by eq. (2.15) a straightforward calculation gives

$$\nabla^a_{n,\mu} S = -\frac{\beta}{2N} \operatorname{Tr} T^a (\chi_{n,\mu} - \tilde{\chi}_{n,\mu}) - \delta_{(n,\mu),L_1} \frac{\operatorname{Tr}(T^a W(L_1)_{n,\mu})}{\operatorname{Tr} W(L_1)_{n,\mu}}$$

$$+ \delta_{(n,\mu),L_2} \frac{\operatorname{Tr}(T^a W(L_2)_{n,\mu})}{\operatorname{Tr} W(L_2)_{n,\mu}}, \tag{2.20}$$

$$\chi_{n,\mu}(U) \equiv \sum_{\nu \neq \mu} \left\{ U^{-1}_{n,\nu} U^{-1}_{n+\hat{\nu},\mu} U_{n+\hat{\mu},\nu} U_{n,\mu} + U_{n-\hat{\nu},\nu} U^{-1}_{n-\hat{\nu},\mu} U^{-1}_{n+\hat{\mu}-\hat{\nu},\nu} U_{n,\mu} \right\}, \tag{2.21}$$

$$\tilde{\chi}_{n,\mu}(U) \equiv \sum_{\nu \neq \mu} \left\{ U^{-1}_{n,\mu} U^{-1}_{n+\hat{\mu},\nu} U_{n+\hat{\nu},\mu} U_{n,\mu} + U^{-1}_{n,\mu} U_{n+\hat{\mu}-\hat{\nu},\nu} U_{n-\hat{\nu},\mu} U^{-1}_{n-\hat{\nu},\nu} \right\}. \tag{2.22}$$

Before discussing the results of our Monte Carlo simulations of (2.16) and (2.19)–(2.22) let us discuss shortly some numerical problems associated with the complex Langevin equation [6, 8, 9]. The actions (2.14) and (2.15) will in general be complex and when θ_ℓ moves into the complex plane and U_ℓ from SU(N) to SL(N, C) the action will not be bounded from below. Consequently, for the noiseless classical part of the Langevin equation, there exist unstable paths along which the variables in question will be taken to infinity within a finite time. The noise term prohibits the occurrence of such a trajectory out to infinity, but from time to time the variable will take quite a large detour away from the stability point, around which it is fluctuating and the numerical value of the drift term will be large during this detour. If we kept the finite step-size Δt (forced upon us in the practical implementation of the differential equation) fixed we would eventually lose control over the stochastic equation, which would degenerate into a deterministic one, in general being a discretized artifact having run-away solutions as generic solutions (see ref. [8] for special examples and details). The problem of instabilities grows with the lattice size as the number of independent variables grows with lattice size. Our updating algorithm has therefore been chosen as the ordinary first-order discretized Langevin equation for each lattice link separately, but with multihit on each link in such a way that the total Langevin time-step forward for that link was equal to a prefixed value Δt. The individual $(\Delta t)_i$ was chosen in such a way that $\Delta\theta_i$ is always less than a fixed number. This algorithm turns out to be quite efficient in dealing with the numerical instabilities. Higher order Runge-Kutta algorithms with fixed Δt did not avoid the numerical instabilities triggered by the large drift term. We have not explored the systematics needed in order to find the optimal algorithm, as the computer time used was not incompatible with such a small choice of $(\Delta t)_{\text{prefixed}}$ (≈ 0.01) that the first-order algorithm is sufficiently precise.

3. U(1) lattice gauge theory in two dimensions: a success

The most obvious test of the method outlined in the last sections is the U(1) gauge theory in two dimensions. It has the simplest structure of all the gauge theories and everything can be calculated analytically. The partition function and action is given by eqs. (2.8) and (2.14). Large β corresponds to the continuum limit ($1/\beta = e^2a^2$, a = lattice spacing, e = coupling constant) and here one has

$$\beta(1 - \cos\theta_\square) \approx \tfrac{1}{2}E^2(x)a^2, \tag{3.1}$$

where $E(x)$ denotes the electric field at plaquette $\square \sim x$. The electric energy density in the presence of external charges can be defined as:

$$\varepsilon(x) \equiv -\tfrac{1}{2}\left[\left\langle E^2(x)\right\rangle_{e^+e^-} - \left\langle E^2(x)\right\rangle_{\text{vacuum}}\right]. \tag{3.2}$$

The overall minus sign in (3.6) is due to the rotation $E \to iE$ in euclidean space.

In the finite volume limit we get for $\langle\cos\theta_\square\rangle$ outside the charges (the Wilson lines) and between the charges (compare fig. 1 with x_1 as spatial coordinate)

$$\langle\cos\theta_\square\rangle_{\text{outside charge}} = I_1(\beta)/I_0(\beta) = \langle\cos\theta_\square\rangle_{\text{vacuum}}, \tag{3.3}$$

$$\langle\cos\theta_\square\rangle_{\text{between charge}} = I_0(\beta)/I_1(\beta) - 1/\beta, \tag{3.4}$$

and from (3.1)–(3.4) we get for the energy density between the charges:

$$\varepsilon(x) = e^2\left[\left(\frac{I_0(\beta)}{I_1(\beta)} - \frac{1}{\beta}\right) - \frac{I_1(\beta)}{I_0(\beta)}\right], \tag{3.5}$$

$$\varepsilon(x) = \tfrac{1}{2}e^2\left(1 + \mathrm{O}(e^2a^2)\right). \tag{3.6}$$

This corresponds, as it should, to an electric field between the charges. Outside the charge we have $\varepsilon(x) = 0$.

In figs. 2 and 3 we show the result of Monte Carlo simulations for various values of β if a 20×21 lattice using bag boundary conditions which corresponds to $\theta_\square = 0$ at the spatial boundary in the case of two dimensions. The physical reason for this choice is clear. If we are not in the infinite volume limit, and the charges are separated by $\frac{1}{2}L$ (L being the linear extension of our lattice) there is no stable ground state configuration if we use periodic boundary conditions. The flux can go either way around the torus. Indeed we have observed this kind of string flipping. Among the other choices of boundary conditions, the bag boundary condition have the nice feature that it forbids the building up of static charges at the boundary and we could actually take the two charges almost to the boundary and still get the right field strength between them.

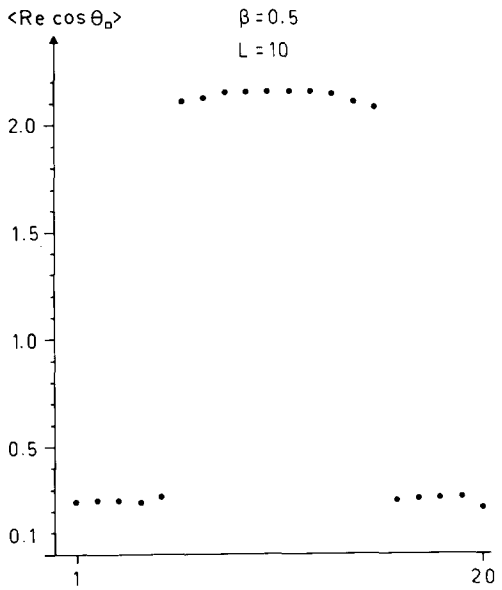

Fig. 2. Measured averages of $\mathrm{Re}\cos\theta_{\square}$ for $\beta = 0.5$ on a 20×21 lattice with the 2 charges separated by 10 lattice spacings. The Langevin iterations were performed with the multihit method described in the text with $\Delta t_{\mathrm{prefixed}} = 0.01$. In total 50 ksweeps were used out of which 30 ksweeps were used for thermalization.

The complex Langevin equation (2.16) has a stability point around which it fluctuates:

$$\theta_{n,1} = 0\,, \qquad \theta_{n,2} = i\Psi_{n,2}\,,$$

$$\Psi_{x,2} = 0 \qquad \text{for } x_1 \leqslant L_1\,,$$

$$\Psi_{x,2} = \left[\sinh^{-1}\left(\frac{1}{\beta}\right)\right](x_1 - L_1) \qquad \text{for } L_1 < x_1 \leqslant L_2\,,$$

$$\Psi_{x,2} = \left[\sinh^{-1}\left(\frac{1}{\beta}\right)\right](L_2 - L_1) \qquad \text{for } x_1 > L_2\,. \tag{3.7}$$

(Of course Ψ is not uniquely defined because the gauge degrees of freedom.)

This stability point corresponds to a linear rising potential between the charges and the complex Langevin equation does not seem to have any difficulty in finding it. It fluctuates around this point and indeed generates the *relevant* configurations. In order to stress the tremendous gain obtained by this method compared to the conventional Wilson line method let us note that it takes only a couple of VAX 11/780 hours to measure the string tension for charges separated by 10 lattice

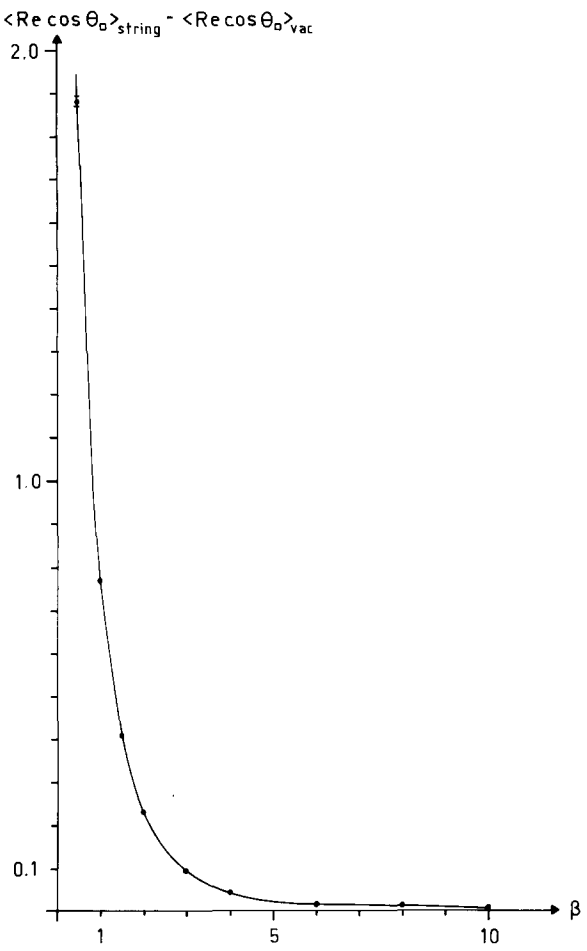

Fig. 3. Measured averages of the differences between $\mathrm{Re}\cos\theta_{\square}$ inside and outside the string for β-values in the range 0.5 to 10 on a 20×20 lattice with the two charges separated by 10 lattice spacings. The choice of Δt as in fig. 2. For all β-values 50 ksweeps were performed. At $\beta = 0.5$, 1.0 and 2.0 30 ksweeps were used for thermalization, whereas 20 ksweeps were used for all other β-values.

spacings on a 20×21 lattice even in the strong coupling region, where $\beta = 0.5$. Using conventional methods one would have to measure a Wilson loop with expectation value $(I_1(\beta))/I_0(\beta))^{10\times 20} = (\text{for } \beta = 0.5)\ 0.6\times 10^{-111}$!! As can be seen from fig. 2 the algorithm is able to account for the one order of magnitude difference between the field strengths between adjacent plaquettes inside and outside the string. The difference between the theoretical value of $\langle\cos\theta_{\square}\rangle$ and the Monte Carlo value as a function of the prefixed time-step Δt is shown in fig. 3 for β-values ranging from 0.5 to 10. The result is impressive! Let us finally mention that we have carefully checked that the average $\langle\cos\theta_{\square}\rangle$ between the charges converge to the correct theoretical value as $\Delta t \to 0$ [4].

4. U(1) in three and four dimensions

Encouraged by the success of the complex Langevin equation for U(1) lattice gauge theory two dimensions we now turn to the less trivial situation in three dimensions. Compact U(1) in three dimensions is still a fairly well understood theory due to the works of Polyakov [10], Banks, Myerson and Kogut [11] and Göpfert and Mack [12]. The magnetic monopoles present in the theory have a Coulomb gas interaction with a stationary electric current loop. This three-dimensional Coulomb gas is always in the plasma phase: the only thing that changes as we vary β is the density of monopoles which goes exponentially to zero with increasing β. However, for any finite value of β it gives rise to a mass gap and a non-zero string tension, which both fall off exponentially with β.

From a numerical point of view the situation is less clear. In [13] the string tension was measured using conventional Wilson loop technique and it was doubtful whether any string tension could be observed in the crossover region to weak coupling (where only the Coulomb part can be seen due to the fact that the string tension is exponentially small). Later measurements [14] using a dual formulation, which unfortunately only works for abelian gauge theories, yield a non-vanishing string tension which disagreed with Polyakov's continuum formula by a factor of 4. It seems hard to believe that one should be so far from the continuum limit near the crossover. The picture is even more confusing since the dual formulation using the Villain action instead of the Wilson action shows nice agreement with Polyakov's formula in the crossover region.

We have measured the energy density in the presence of static charges for compact U(1) using the complex Langevin equation (2.16). The energy density is defined as in (3.2) only do we have instead of (3.1):

$$e^2 a = \frac{1}{\beta}, \tag{4.1}$$

$$\beta(1 - \cos\theta_{\square}) \approx \tfrac{1}{2} F_{\mu\nu}^2(x) a^3, \tag{4.2}$$

$$\begin{aligned} \varepsilon(x) = -\tfrac{1}{2}\Big[&\big\langle \boldsymbol{E}^2(x)\big\rangle_{e^+e} - \big\langle \boldsymbol{E}^2(x)\big\rangle_{\text{vacuum}} \\ &- \big\langle B^2(x)\big\rangle_{e^+e} + \big\langle B^2(x)\big\rangle_{\text{vacuum}}\Big]. \end{aligned} \tag{4.3}$$

In eq. (4.2) there is no summation over repeated indices and $r, \mu \in \square$. In eq. (4.3) we have to include the magnetic field because the string between the charges can vibrate and therefore induce a magnetic field. We can now define

$$\begin{aligned} \varepsilon(x) = +\frac{1}{2}\frac{\beta}{a^3}\Big[&\big(\langle\cos\theta_{(1,3)}\rangle_{e^+e} - \langle\cos\theta_{(1,3)}\rangle_{\text{vacuum}}\big) \\ &+ \big(\langle\cos\theta_{(2,3)}\rangle_{e^+e} - \langle\cos\theta_{(2,3)}\rangle_{\text{vacuum}}\big) \\ &- \big(\langle\cos\theta_{(1,2)}\rangle_{e^+e} - \langle\cos\theta_{(1,2)}\rangle_{\text{vacuum}}\big)\Big] \end{aligned} \tag{4.4}$$

and use this as a definition of ε even in the strong coupling region. A strong coupling expansion shows that $\varepsilon(x) \sim 1/\beta$ on the minimal surface connecting the two Wilson lines and that it goes to zero as $O(\beta)$ outside this sheet.

We have measured $\varepsilon(x)$ and the separate components of $\varepsilon(x)$ in eq. (4.4) by use of the complex Langevin equation. In the weak coupling region ($\beta > 2.2$) the Langevin equation works very well. For $\beta > 2.2$ the string tension is so small that we should only see a Coulomb field around the charges (a dipole field), and indeed we do. In fig. 4 a typical measurement is displayed. Two Coulomb peaks can clearly be identified. We feel confident that the method works in this region, where there exist a well-defined stability point corresponding to a classical dipole field around which the variable θ_ℓ fluctuates. As in the two-dimensional case this stability point is purely imaginary. We can use the imaginary part of the r.h.s. of eq. (2.16) as a measure of how well the stability point is found. It does not depend *explicitly* on the (real) noise and if it is zero it means that $\mathrm{Im}(\Delta\theta_\ell) = 0$. As shown in fig. 5 there is an abrupt change in $\langle \mathrm{Im}(\Delta\theta_\ell) \rangle$ when we leave the weak coupling region. There is nothing wrong with this: the same phenomena occurs in the two-dimensional case. The difference is that when we move into the strong coupling region there *is* no stability point in three dimensions corresponding to the one in the two-dimensional case, where the strong coupling dominates the sheet between the Wilson lines. This sheet is just the classical solution in the two-dimensional case. Maybe it is this lack of stability point that is responsible for the fact that the strong coupling region of the three-dimensional theory seems to be wrongly simulated by the complex

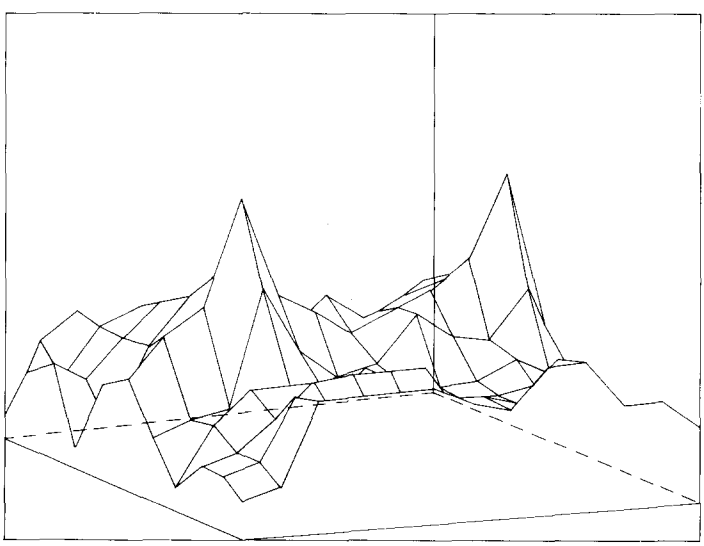

Fig. 4. Typical electric field energy distribution at weak coupling ($\beta = 3.0$). The charges are 8 lattice spacings apart.

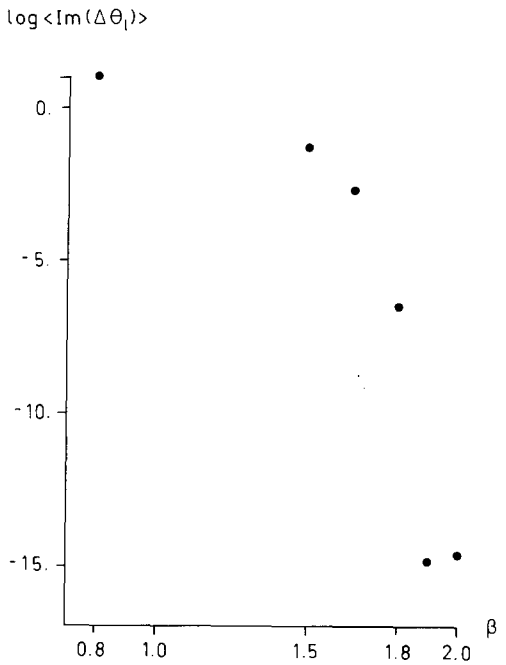

Fig. 5. The imaginary part of the drift term, the r.h.s of eq. (2.16), for a temporal link $\theta_\ell \in U(1)_3$. It measures the fluctuations around the classical saddle-point. Only one configuration has been averaged. For $\beta > 1.6$–1.8 the classical solution dominates.

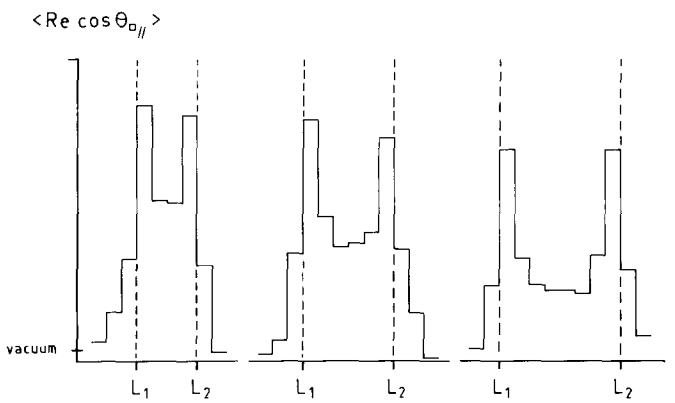

Fig. 6. $\langle \mathrm{Re} \cos \theta_\square \rangle$ for the plaquette along the string axis through the Wilson lines at L_1 and L_2 for compact U(1) in 3 dimensions at $\beta = 1.2$. L_1 and L_2 are chosen such that $|L_1 - L_2| = 4$, 6 and 8 on lattice sizes 9^3, 12^3 and 12^3 respectively. All runs were made with $(\Delta t)_{\text{prefixed}} = 0.1$. In each case 10 ksweeps were used for thermalization and 30 ksweeps for measurements.

Langevin equation. At least we have to conclude that the method do not give the correct string tension in this case. Although the electric field between the charges is clearly seen for strong coupling, it is not constant and cannot be identified with a string. Also the field strengths do not grow as $1/\beta$ which is expected from strong coupling arguments. This failure is illustrated in fig. 6, where the central part of the energy density, E^2, is shown for $\beta = 1.2$ for 3 different charge separations. No constant energy density is observed.

In the crossover region between strong and weak coupling we have found a small indication of a string between the charges but the expected magnitude of the string tension at this β-value is certainly less than what came out from the simulations using the dual algorithm [14]. It is not clear however that the dual algorithm gives the correct answer as discussed above. The sad conclusion of this section is that the algorithm cannot be trusted in the strong coupling regime and as we do not know precisely where and why it fails, it must be discarded. Similar statements hold for U(1) in four dimensions: In the Coulomb phase the algorithm seems to work well but moving towards strong coupling it gives wrong results.

5. Quantum mechanical disasters of the first degree

For the non-abelian gauge theories the situation is at least as bad as in two- and three-dimensional U(1) at strong couplings. This can be explicitly illustrated by a simple quantum mechanical example taken from the abelian theory in two dimensions. In the case of two-dimensional U(1) we simulated (by factorization of the theory) essentially the one-dimensional partition function: ($\theta \equiv \theta_{\square}$)

$$S = \beta \cos\theta + i\theta \tag{5.1}$$

and we were interested in averages of the form:

$$\langle \cos\theta \rangle_S = \frac{\int \mathrm{d}\theta \cos\theta \exp(\beta \cos\theta + i\theta)}{\int \mathrm{d}\theta \exp(\beta \cos\theta + i\theta)} . \tag{5.2}$$

We could as well write eqs. (5.1) and (5.2) as:

$$S = \beta \cos\theta + \log(\cos\theta), \tag{5.3}$$

$$\langle \cos\theta \rangle_S = \frac{\int \mathrm{d}\theta \cos\theta \exp(\beta \cos\theta + \log(\cos\theta))}{\int \mathrm{d}\theta \exp(\beta \cos\theta + \log(\cos\theta))} . \tag{5.4}$$

In a certain sense eq. (5.3) is more analogous to the non-abelian case than eq. (5.1) as is apparent from eq. (2.15). However, as will be demonstrated below, *the complex Langevin gives wrong results in the strong coupling regime of* (5.3).

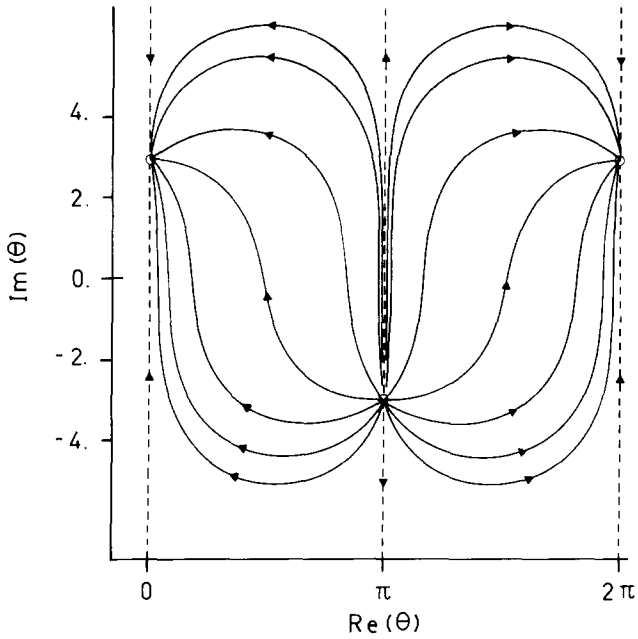

Fig. 7. Flow pattern for U(1) (i.e. trajectories traced out by Langevin eq. without noise term η) with action $S = -\beta \cos\theta + i\theta$ for $\beta = 0.1$.

The Langevin equation corresponding to eq. (5.3) is given by

$$\dot{\theta} = -\beta \sin\theta - \operatorname{tg}\theta + \eta . \tag{5.5}$$

For $\beta < 1$ the flow diagram corresponding to this equation is shown in fig. 8. It is seen that θ is always attracted towards the real axis and once it is in the neighbourhood of the real axis it cannot move away as long as the noise term η is real. Consequently the expectation value of $\cos\theta$ do not behave like $1/\beta$ as $\beta \to 0$. That would require θ to move far out in the complex plane. This is indeed what happens with the action in eq. (5.1) as can be seen in fig. 7 where the flow diagram corresponding to eq. (5.1) is shown.

As can be seen in fig. 9 the flow diagram changes its nature for $\beta > 1$. Actually $\operatorname{Im}\theta \to 0$ for all values of β. For large β the Langevin equation (eq. (5.5)) works correctly. The same conclusions are true for non-abelian analogs to eq. (5.3):

$$S(U) = \beta \operatorname{Tr} U + \ln \operatorname{Tr} U . \tag{5.6}$$

In fig. 10 $\langle \operatorname{Re}\cos\theta \rangle$ is shown for U(1) with the action of eq. (5.3) using the Langevin equation (eq. 5.5)). Also shown is the same quantity without the source term ($\ln\cos\theta$). For comparison the exact analytic solutions are also displayed. For

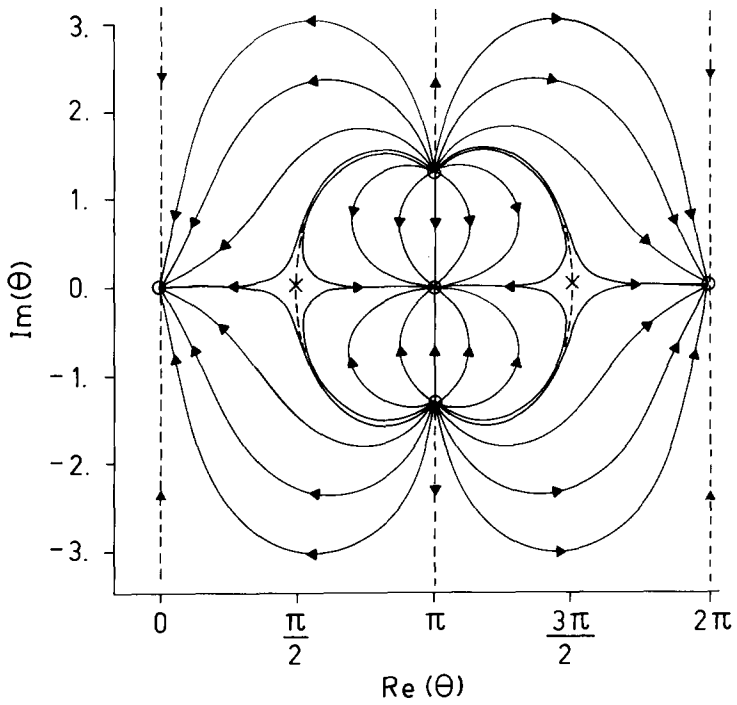

Fig. 8. Flow pattern with action $S = \beta \cos\theta + \log(\cos\theta)$ for $\beta = 0.5$. The fixed points encountered outside the real axis for $\beta < 1$ are denoted (0). Singularities (i.e. points of zero probability measure) from the source-term exist at $\theta = \frac{1}{2}\pi \bmod \pi$.

U(1) these are given by eqs. (3.3) and (3.4) respectively. In figs. 11 and 12 the corresponding quantities, $\frac{1}{2}\langle \mathrm{Re\,Tr}\, U\rangle$ and $\frac{1}{6}\langle \mathrm{Re\,Tr}(U + U^{-1})\rangle$, are shown for SU(2) and SU(3) respectively using the action of eq. (5.6) with the complex Langevin equation (cf. eqs. (2.15) and (2.16)). Also shown in figs. 11 and 12 are the exact analytic solutions for SU(N) which are obtained from [15]

$$Z(\beta, N) \sim \int_0^{2\pi} \prod_1 \mathrm{d}\alpha_i \, |\det \Delta|^2 \exp\left(\frac{\beta}{N} \sum_{i=1}^{N} \cos\alpha_i\right), \tag{5.7}$$

with

$$\Delta_{j,k} = \mathrm{e}^{i(j\alpha_k)}.$$

By forming $\delta_\beta Z/Z$ and $\delta_\beta^2 Z/\delta_\beta Z$ one obtains for $N = 2$

$$\tfrac{1}{2}N\langle \mathrm{Re\,Tr}(U + U^{-1})\rangle = \begin{cases} I_1(\beta)/I_2(\beta) - 3/\beta & \text{(with source)} \\ I_2(\beta)/I_1(\beta) & \text{(without source)} \end{cases}, \tag{5.8}$$

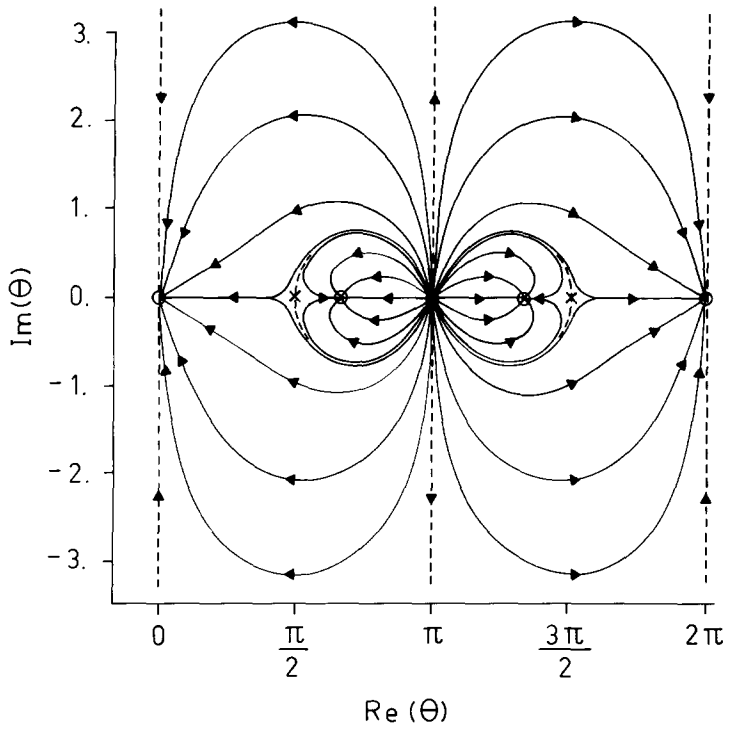

Fig. 9. Flow pattern as in fig. 8 but with $\beta = 2$. No imaginary fixed points occur in this case.

whereas for SU(3) numerical evaluations of the derivatives of eq. (5.7) are necessary. The effect of the $\beta \to 0$ properties of the flow diagrams in figs. 7–9 are striking in figs. 10–12. On the other hand, very correct results are obtained in the weak coupling sector. As an example consider the difference between the full and sourceless part of the SU(2) case at $\beta = 10$ where the Langevin prediction is $= 0.0171(10)$ as compared with the exact result 0.0165.

We conclude that the complex Langevin equation does not give the correct $\beta \to 0$ physics for these simple U(1), SU(2) and SU(3) quantum mechanical toy models, whereas it works well in the weak coupling region.

6. Non-abelian disasters of third degree

The results of sect. 4 and 5 did not leave much hope that the complex Langevin equation would work for the strong coupling regime when simulating the non-abelian gauge theory using the action (2.15).

Still, the interesting physics takes place for large β, near the continuum limit and all examples mentioned up to now worked for large β. In addition the non-abelian

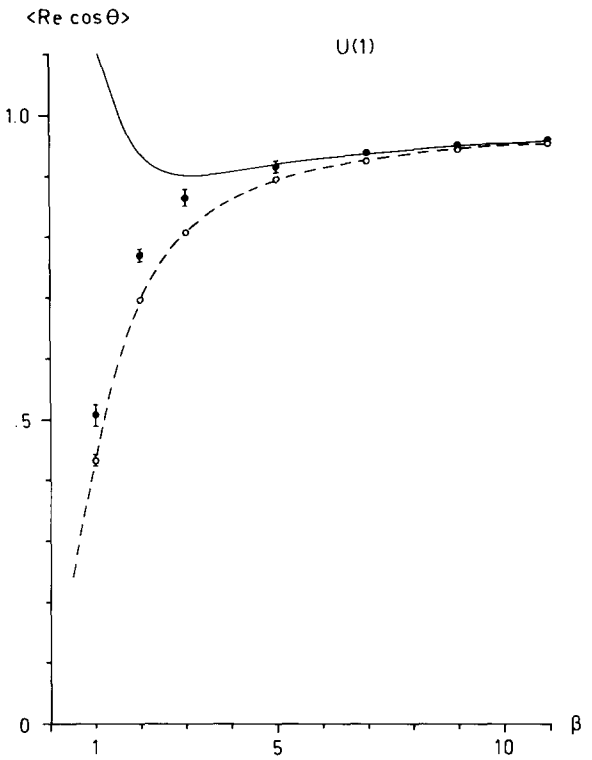

Fig. 10. $\langle \mathrm{Re}\cos\theta \rangle$ from Langevin simulations of eq. (5.3). The filled circles correspond to eq. (5.3) whereas the open circles were obtained with no source-term in the action. The corresponding analytic solutions (eqs. (3.3) and (3.4)) are represented by a full and a dashed line respectively. The errors are less than the circles when not explicitly drawn. $\langle \mathrm{Im}\cos(\theta) \rangle$ are very small and within the errors of the real parts. In total 5×10^5 sweeps were used with $\Delta t = 0.005$.

theories do not factorize even in two dimensions in contrast to the abelian case and hence the conclusions of sect. 5 are not a priori forced upon us in a stringent way.

The "factorization" of the non-abelian theory comes about as follows: we assume that we have the situation shown in fig. 1 and use the freedom of gauge fixing to fix all link matrices in the spatial direction to be 1. The partition function of eq. (2.16), $Z(\beta, L_1, L_2)$, is then given by

$$Z(\beta, L_1, L_2) = \int \prod_n \mathrm{d}U_{n,2} \frac{1}{N} \mathrm{Tr}\, W(L_1) \frac{1}{N} \mathrm{Tr}\, W(L_2)^{-1} \times \exp\left[\frac{\beta}{2N} \sum_n \mathrm{Tr}\left(U_{n,2}^{-1} U_{n+\hat{1},2} + U_{n+\hat{1},2}^{-1} U_{n,2} \right) \right]. \tag{6.1}$$

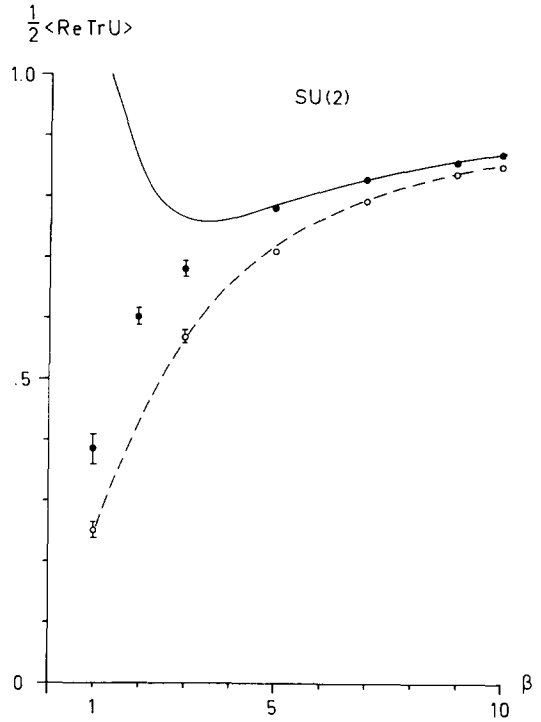

Fig. 11. $\frac{1}{2}\langle \mathrm{Re}\,\mathrm{Tr}\,U\rangle$ for SU(2) from Langevin simulations of the one-dimensional quantum mechanical analogue of eq. (5.6). Same notation as in fig. 10. The analytic solutions (full and dashed lines) were obtained from eq. (5.8). In total 5×10^5 sweeps were used with $\Delta t = 0.005$.

The Haar measure on SU(N) is invariant under the change of variables

$$U_{n,2} \to V_n = U_{n,2}U^{-1}_{n+\hat{1},2}\,. \tag{6.2}$$

This is the analogue of the change $\theta_\ell \to \theta_\square$ the abelian case. The difference is that while $\theta_\square$ is gauge invariant ($F_{\mu\nu}$ is gauge invariant in an abelian theory), V can still be gauged by

$$V_n \to W_n V_n W_n^{-1}\,, \tag{6.3}$$

where W_n only varies in the time direction. The partition function (eq. (6.1)) is

$$Z(\beta, L_1, L_2) = \int \prod_n \mathrm{d}V_n \frac{1}{N}\mathrm{Tr}\left[\prod_{n\in L_1}\left(\prod_{k=0,\,L_1-L_2} V_{n+\hat{1}k}\right)\right]$$
$$\times \frac{1}{N}\mathrm{Tr}\left[\prod_{n\in L_2}\left(\prod_{k=0,\,L_1-L_2}(V_{n+\hat{1}k})^{-1}\right]\exp\left[\frac{\beta}{2N}\sum\left(\mathrm{Tr}\,V_n + \mathrm{Tr}\,V_n^{-1}\right)\right],\right. \tag{6.4}$$

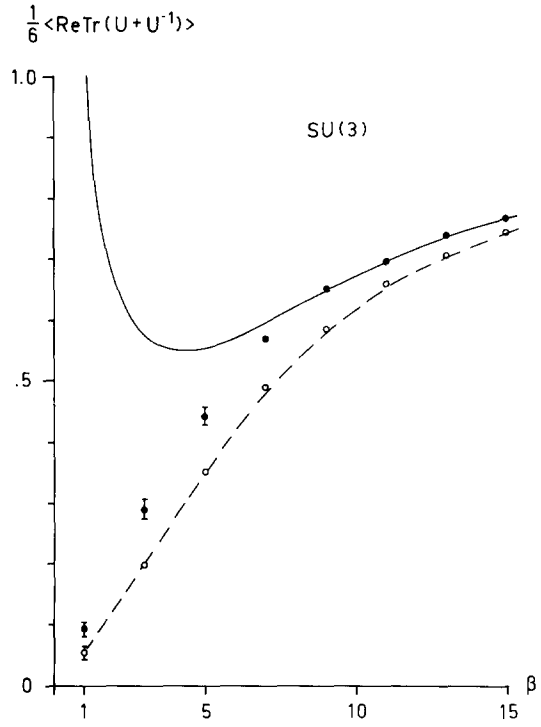

Fig. 12. $\frac{1}{6}\langle \mathrm{Re}\,\mathrm{Tr}(U+U^{-1})\rangle$ for SU(3) from Langevin simulations of the one-dimensional quantum mechanical analogue of eq. (5.6). Same notation as in fig. 10. The analytic solutions (full and dashed lines) were obtained by numerical integrations of the derivatives of eq. (5.7). In total 5×10^5 sweeps were used with $\Delta t = 0.005$.

where L is the spatial extension of the lattice. For n being on the l.h.s. of L (see fig. 1) the integral factorizes since it is just a product of single plaquette integrals.

$$Z(\beta) = \int \mathrm{d}V \exp\left[\frac{\beta}{2N}(\mathrm{Tr}\,V + \mathrm{Tr}\,V^{-1})\right]. \tag{6.5}$$

For n being between L_1 and L_2 we get integrals of the type

$$\int \mathrm{d}V \frac{1}{N}\mathrm{Tr}\,VA \exp\left[\frac{\beta}{2N}(\mathrm{Tr}\,V + \mathrm{Tr}\,V^{-1})\right]$$

$$\neq \frac{1}{N}\mathrm{Tr}\,A \int \mathrm{d}V\,\mathrm{Tr}\,V \exp\left[\frac{\beta}{2N}(\mathrm{Tr}\,V + \mathrm{Tr}\,V^{-1})\right]. \tag{6.6}$$

Hence the integral in eq. (6.4) does not factorize explicitly but successive integrations yield

$$Z'(\beta)^{T(L_2-L_1)}, \tag{6.7}$$

where

$$Z'(\beta) = \int dV \frac{1}{N} \mathrm{Tr}\, V \exp\left[\frac{\beta}{2N}(\mathrm{Tr}\, V + \mathrm{Tr}\, V^{-1})\right] \tag{6.8}$$

is just the quantum mechanical toy example considered in sect. 5 (eq. (5.6)). Finally, for n on the r.h.s of L_2 we obtain integrals of the type

$$\int dV \frac{1}{N} \mathrm{Tr}\, VA \frac{1}{N} \mathrm{Tr}\, B^{-1} V^{-1} \exp\left[\frac{\beta}{2N}(\mathrm{Tr}\, V + \mathrm{Tr}\, V^{-1})\right]$$

$$\neq \frac{1}{N} \mathrm{Tr}\, A \frac{1}{N} \mathrm{Tr}\, B^{-1} \int dV \exp\left[\frac{\beta}{2N}(\mathrm{Tr}\, V + \mathrm{Tr}\, V^{-1})\right], \tag{6.9}$$

and again successive iterations lead to a factor of the type in eq. (6.5).

As mentioned above the lack of explicit factorization in the partition function before integration does not force the results of sect. 5 upon us in the non-abelian case. And indeed they are *not* reproduced by the simulation of SU(2) and SU(3) with non-abelian charges. Unfortunately the situation is even worse! We do not see any sign of an energy density built up between the charges and have to conclude that the method does not work in this case!

7. Discussion

We have discussed in detail the application of the complex Langevin equation to physical systems of great interest: lattice gauge theories with static charges included in the action. The results obtained illustrates both the potential tremendous power of the method, and its limitations. The power of the method is apparent in the simulation of two-dimensional U(1). It is possible to penetrate into regions of the theory which are totally inaccessible by conventional methods. This success is not confined to rather trivial systems like U(1) gauge theory in two dimensions. In ref. [6] the complex Langevin equation was also applied to the chiral SU(N) model in an external field. Here the action is also complex and again it was possible to address questions inaccessible by conventional methods.

However the method can fail. It does not have the same range of general applicance as conventional Monte Carlo methods. At this moment we do not understand the algorithm sufficiently well to be able to predict when the method can be applied or not to a specific problem. In some cases the potential gain is so large that it is worthwhile to test its applicability. Then it is preferable to have as test variables some observables that can be computed by conventional methods. If in such a case one has agreement between the measurements of these variables one can say with a great deal of confidence that the complex Langevin equation works

in this particular case. This point is nicely illustrated in the chiral SU(N) model in an external field [6]. The Noether charge associated with the external field is impossible to measure with conventional methods in the large-volume strong field region. However, the neighbour-spin correlation function can be measured by both methods and the results agree well.

Note added in proof

After the completion of this work we received a paper [16] attacking the same problem with similar conclusions.

References

[1] H. Hüffel and H. Rumph, Phys. Lett. 148B (1984) 104;
E. Gozzi, Phys. Lett. 150B (1985) 119;
H. Hüffel and P.V. Landshoff, Nucl. Phys. B260 (1985) 545;
D.V.E. Callaway, F. Cooper, S.R. Klauder and H.A. Rose, Nucl. Phys. B262 (1985) 19;
H. Nakazato and Y. Yamanaka, Phys. Rev. D34 (1986) 492
[2] J.R. Klauder, Phys. Rev. A29 (1984) 2036
[3] G. Bhanot, E. Rabinovici, N. Seiberg and P. Woit, Nucl. Phys. B230 [FS10] (1984) 291;
G. Bhanot, R. Dashen, N. Seiberg and H. Levine, Phys. Rev. Lett. 53 (1984) 519
[4] J. Ambjørn, M. Flensburg and C. Peterson, Phys. Lett. 159B (1985) 335
[5] S.-K. Yang, Nucl. Phys. B267 (1986) 290
[6] J. Ambjørn and S.-K. Yang, Nucl. Phys. B275 [FS17] (1986) 18
[7] G. Parisi, Phys. Lett. 131B (1983) 393
[8] J. Ambjørn and S.-K. Yang, Phys. Lett. 165B (1985) 140
[9] J.R. Klauder and W.P. Petersen, J. Stat. Phys. 39 (1985) 53
[10] A.M. Polyakov, Nucl. Phys. B120 (1977) 429
[11] T. Banks, R. Myerson and J. Kogut, Nucl. Phys. B129 (1977) 493
[12] M. Göpfert and G. Mack, Commun. Math. Phys. 82 (1982) 545
[13] J. Ambjørn, A.J.G. Hey and S. Otto, Nucl. Phys. B210 [FS6] (1982) 347
[14] T. Sterling and J. Greensite, Nucl. Phys. B220 [FS8] (1983) 327;
M. Karliner and G. Mack, Nucl. Phys. B225 [FS9] (1983) 371;
C. Peterson and L. Sköld, Nucl. Phys. B255 (1985) 365
[15] D.J. Gross and E. Witten, Phys. Rev. D21 (1980) 446
[16] J. Flower, S.W. Otto and S. Callahan, Caltech preprint CALT-68-1339 (1986)